Realistic Spiking Neural Network: Non-synaptic Mechanisms Improve Convergence in Cell Assembly

Damien Depannemaecker, Luiz Eduardo Canton Santos, António Rodrigues, Carla Alessandra Scorza, Fulvio Alexandre Scorza, Antônio-Carlos Guimarães de Almeida

Journal Pre-proof

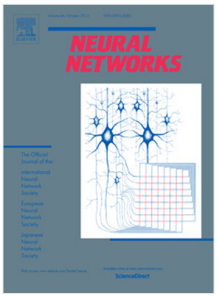

Realistic Spiking Neural Network: Non-synaptic Mechanisms Improve Convergence in Cell Assembly

Damien Depannemaecker, Luiz Eduardo Canton Santos, Antônio Márcio Rodrigues, Carla Alessandra Scorza, Fulvio Alexandre Scorza, Antônio-Carlos Guimarães de Almeida

PII: S0893-6080(19)30320-X
DOI: https://doi.org/10.1016/j.neunet.2019.09.038
Reference: NN 4289

To appear in: *Neural Networks*

Received date : 22 February 2019
Revised date : 17 September 2019
Accepted date : 23 September 2019

Please cite this article as: D. Depannemaecker, L.E.C. Santos, A.M. Rodrigues et al., Realistic Spiking Neural Network: Non-synaptic Mechanisms Improve Convergence in Cell Assembly. *Neural Networks* (2019), doi: https://doi.org/10.1016/j.neunet.2019.09.038.

Realistic Spiking Neural Network: Non-synaptic Mechanisms Improve Convergence in Cell Assembly

Authors: Depannemaecker, Damien[1,2]; Canton Santos, Luiz Eduardo[1,2]; Rodrigues, Antônio Márcio[1]; Scorza, Carla Alessandra[2]; Scorza, Fulvio Alexandre[2]; Almeida, Antônio-Carlos Guimarães de[1,*]

[1]Laboratório de Neurociência Experimental e Computacional, Departamento de Engenharia de Biossistemas, Universidade Federal de São João del-Rei (UFSJ), Brazil

[2]Disciplina de Neurociência, Departamento de Neurologia e Neurocirurgia, Universidade Federal de São Paulo (UNIFESP), São Paulo, Brazil

Corresponding Author:

Antônio-Carlos Guimarães de Almeida, Lanec/DEPEB/UFSJ

Pr. Dom Helvécio, 74

São João del-Rei – MG – 36.301-160, BRAZIL

E-mail address: acga@ufsj.edu.br

Phone number: +55 32 3379 5568

Fax number: +55 32 3379 3104

Realistic Spiking Neural Network: Non-synaptic Mechanisms Improve Convergence in Cell Assembly

Authors: Depannemaecker, Damien[1,2]; Canton Santos, Luiz Eduardo[1,2]; Rodrigues, Antônio Márcio[1]; Scorza, Carla Alessandra[2]; Scorza, Fulvio Alexandre[2]; Almeida, Antônio-Carlos Guimarães de[1,*]

[1]Laboratório de Neurociência Experimental e Computacional, Departamento de Engenharia de Biossistemas, Universidade Federal de São João del-Rei (UFSJ), Brazil

[2]Disciplina de Neurociência, Departamento de Neurologia e Neurocirurgia, Universidade Federal de São Paulo (UNIFESP), São Paulo, Brazil

Corresponding Author:

Antônio-Carlos Guimarães de Almeida, Lanec/DEPEB/UFSJ

Pr. Dom Helvécio, 74

São João del-Rei – MG – 36.301-160, BRAZIL

E-mail address: acga@ufsj.edu.br

Phone number: +55 32 3379 5568

Fax number: +55 32 3379 3104

Abstract: Learning in neural networks inspired by brain tissue has been studied for machine learning applications. However, existing works primarily focused on the concept of synaptic weight modulation, and other aspects of neuronal interactions, such as non-synaptic mechanisms, have been neglected. Non-synaptic interaction mechanisms have been shown to play significant roles in the brain, and four classes of these mechanisms can be highlighted: i) electrotonic coupling; ii) ephaptic interactions; iii) electric field effects; and iv) extracellular ionic fluctuations. In this work, we proposed simple rules for learning inspired by recent findings in machine learning adapted to a realistic spiking neural network. We show that the inclusion of non-synaptic interaction mechanisms improves cell assembly convergence. By including extracellular ionic fluctuation represented by the extracellular electrodiffusion in the network, we showed the importance of these mechanisms to improve cell assembly convergence. Additionally, we observed a variety of electrophysiological patterns of neuronal activity, particularly bursting and synchronism when the convergence is improved.

1. Introduction

Each brain is unique. In each group of neurons with a specific architecture, each neuron has its own specificity. Most living beings with a nervous system are able to quickly distinguish the difference between two types of stimuli from the external world. Depending on the species, senses, sensitivity, and acuity are different. Their survival depends on rapid learning for rapid recognition. During development, the nervous system must be able to adapt very quickly and be responsive to several stimuli. To achieve this aim, groups of cells must be able to specialize, organizing themselves to provide a response (or absence of a response) to a particular stimulus. This procedure involves putting into action a nerve signal projecting into a group of cells for processing of the information.

Donald Hebb introduced the concept of cell assemblies(1). A cell assembly consists of a few dozen neurons(2), characterized by a spatial (network) and temporal (dynamics) structure, which by means of feed forward connections treats and transmits information. The cell assemblies concept is concomitant with the concept of parallel distributed processing (PDP). Rumelhart et al. (3) assumed that neural processing is due to *"interactions between units which excite and inhibit each other in parallel rather than sequential operations"*. Processing and storage of information is not performed by localized structures but is distributed throughout the network. In this sense, cell assemblies are PDP systems but can also be considered as the building blocks for a large-scale PDP system. Cell assemblies are building blocks of brain circuits (4).

In artificial neural networks, the biophysical details of the neurons are neglected in order to be computationally more effective. However, works have been conducted to show the importance of biophysical features at different scales(5,6). In fact, biophysical complexity may play an important role in information processing. In the brain, the information is propagated and exchanged thanks to the variation of the membrane potential of the neurons. Neurons can exhibit a large repertoire of electrophysiological behaviors. Depending on the origin and on the conditions, the information will be coded in different ways, which are called the neural code. A neural code can be based on temporal features, as has been shown for the auditory cortex(7). Another possibility of neural code is to be based on spatial features, as has been observed in the visual cortex (8) and in the hippocampus (9).

Regular spiking and bursting (a sequence of action potentials elicited in quick succession), typical of rhythmic neural synchronization (10), participate in the neural code and may play different roles depending on the brain region; this sequence may also play roles in pathological conditions such as seizures, as observed in epilepsy, and in spreading depression. Many investigations are based on spiking neural networks (SNN) and present binary (spiking/non-spiking) activities. However, time scales are important, and spike coding presents limitations(11). Bursting can make weak synapses reliable(12,13)and may also participate in synaptic plasticity in the cerebellum and hippocampus(13). These features are not only due to synaptic plasticity; neuronal behavior is also influenced by non-synaptic interactions(14,15).

Cell assemblies are not just a PDP system: in response to external stimuli, their activities modify biophysical and biochemical processes in the brain. These changes can be retained longer and express memory properties that constitute an engram. Therefore, the engram is intrinsically related to the PDP activities performed by the cell assemblies.

Adjustments in the neuronal interconnection strength leads to a convergence to produce responses to specific stimuli (16). The responses remain constant over time and, therefore, constitute a memory process. The non-synaptic mechanisms play a role in the biophysical processes involved in the changes in neuronal interconnection strength. Thus, non-synaptic mechanisms has been shown to be influential in the learning and memory processes (17–19).

The complexity of neural tissue not only comes from the high number of substances and mechanisms but also from variability in the tissue. This variability exists as much in the dynamics of the processes as in the local geometry of the tissues. However, despite this variability, different brains from different animals are able to treat the same information to give similar responses or to produce similar endogenous electrophysiological patterns. During the two last decades, approaches in computational modeling have been developed to capture this variability. At a small network scale, investigations (20) have shown that similar to brain regions many different neural network models can produce similar activities patterns. Therefore, brain regions can be modeled while also taking into account intrinsic variability.

The hippocampus, which is a brain region involved in many processes of the brain (21,22), plays an important role in cognition (23,24). For this purpose, the hippocampal cell assemblies provide a spatial and temporal encoding of information (25,26). However, the hippocampus is also one of the brain regions where pathological patterns are observed (27). Seizures, the electrophysiological pattern observed in epilepsy, can be measured at levels ranging from single neurons (28–30) to the entire brain (31,32). Seizures are characterized by synchronous activities and high excitability. Recent works have pointed out the link between synaptic plasticity and epilepsy (33,34) and the effect of such pathology on cognition (35).

Neural networks for machine learning were originally inspired by biological neurons (36,37). Now considered as the third generation of artificial neural networks, spiking neural networks have demonstrated their performance for machine learning applications(38) and especially for computer vision (39). These improvements are due to the use of networks closer to a biological nervous system, considering spiking activities, which permit efficient coding and fast processing of information (40). Specific dynamics such as bursting neurons can also be considered (41). Therefore, a link between neuroscience and neural networks for machine learning applications requires discussing important concepts of the intrinsic properties of different types of networks (40,42).

In this work, we aimed to describe a realistic spiking neural network (RSNN) resembling a hippocampus neural assembly, while also considering the non-synaptic mechanisms present in the region, aiming at investigating

how these realistic descriptions favor the ability to improve learning and synchrony and even promote epileptogenesis. First, computational frameworks to generate RSNNs were built based on biophysical models of neural tissue, including synaptic and non-synaptic interactions between neurons. The models of neural tissue and synaptic communication were based on the previous works from our group(14,43). With simple learning rules, it is shown that the RSNN can converge to solve simple nonlinear tasks. Each RSNN is generated and initialized with different connectivity and different neuronal properties. A crucial influence of non-synaptic interactions was observed.

These observations suggest the importance of two levels of interaction between neurons at two different spatial scales: synaptic and non-synaptic. To investigate whether the observed properties emerge in a network with more simplified neuronal representation, therefore indicating it is feasible to achieve more simplified neural network applications, networks of phenomenological neurons were constructed using the neural model proposed by Izhikevich (44). With similar rules for learning, we observed the ability of such a network to converge to solve simple nonlinear tasks and simple pattern recognition.

To test the robustness of these findings, larger networks were implemented to solve more complex pattern recognition tasks. This investigation allows for evaluating the importance of electrophysiological behaviors (spiking and bursting) and the effect of non-synaptic interactions. The synchronisms observed in the implemented networks and the

corresponding ability to converge were also investigated and interpreted based on neurophysiological evidence. With a neuroscience background, our work aims at offering a new approach, by using a detailed biophysical model, to determine relevant mechanisms in learning and to discuss possible directions to implement it into a neural network for machine learning applications.

2. Methods

The RSNNs used in this work were based on a model of the neurons developed by (14), and the neurotransmission was based on the model developed by(43). The code was written in Fortran90 and run on a high-performance computer (Cluster SGI UV 2000, 80 Cores—Intel Xeon E5-4650v2 10-core, 2.4 GHz, 25MB Cache, RAM 1024GB DDR31866 MHz, 80TB HD, SUSE Linux Enterprise Server 11, SGI Performance Suite, Intel Cluster Studio XE).

The structure of the network layers was based on the morphology of the CA1 region of the hippocampus. In Figure 1A is shown a confocal image stained with fluorescent dyes to distinguish neurons, interneurons and the sequential layers of neurons. Based on this information, we performed the typical cell assembly forming a RSNN.

Identified in Figure 1B and 1C, pyramidal neurons, interneurons and extracellular spaces were represented mathematically as previously described

(14,45). The pyramidal neurons were disposed in layers as suggested by Figure 1A, with the corresponding interconnections categorized in Figure 1B and schematically represented in Figure 1C. An interneuron connects to all layers, receiving input from the first layer of neurons and sending connections to all others.

The cell body of each pyramidal or interneuron neuron is assumed to be a sphere placed in a cubic compartment. Membrane potentials of neurons were calculated using the Goldman-Hodgkin-Katz equation. Ionic concentration changes in the intracellular and extracellular space due to ionic fluxes through ion channels, Na/K-ATPases, cotransporters (KCC, NKCC), and exchangers modify the extracellular space of each neuron, and each of these changes modifies the surrounding extracellular space via electrodiffusion (ED) (Figure 2.a and 2.b). All of these mechanisms were calculated and constitute an important non-synaptic interconnection mechanism. A model of synaptic neurotransmission (Figure 2.c) was implemented following the model previously proposed (43). All parameters values were taken from a literature review (46).

In the next sections, the corresponding models are described. Then, the phenomenological models for the neurons are detailed. It is also shown how networks were generated for both frameworks. Finally, the specific learning rules used in the investigation are described.

2.1. Neurons: Somas of the pyramidal neurons were assumed as a sphere immersed in an extracellular space and are influenced by the activity of the

neighboring neurons. Intracellular and extracellular volumes were estimated by:

$$Vol_{intra} = \frac{4}{3} p R_{cell}^3 \quad (1)$$

$$Vol_{extra} = F_{vol}.Vol_{intra}, \quad (2)$$

where, R_{cell} is the cell radius fixed to 10 µm. The cell membrane surface was estimated by:

$$S_{cell} = 4.p.R_{cell}^2 \quad (3)$$

The membrane potential V_m for each neuron was calculated using the modified Goldman-Hodgkin-Katz equation:

$$V_m = \frac{RT}{F} Ln \frac{p_{Na}[Na^+]_o + p_K[K^+]_o + p_{Cl}[Cl^-]_i + E_{ef} + p_p[A^+]_o + I_{inj}}{p_{Na}[Na^+]_i + p_K[K^+]_i + p_{Cl}[Cl^-]_o + 2 + p_p[A^+]_i}, \quad (4)$$

where $[ion]_i$ and $[ion]_o$ are respectively the intra- and extracellular ion concentration in mM. The Regnault constant is $R = 8.314 V.C.K^{-1}.mol^{-1}$, the temperature is $T = 310$ K. The Faraday constant is $F = 96.487 C.mmol^{-1}$. The effect of electric field E_{ef} is described in the next subsection. Ionic permeability is calculated as follows.

Sodium channels

$$p_{Na} = P_{Na} m^3 h + p_{Na,com} \quad (5)$$

where $p_{Na,com}$ due to the synaptic communication is determined according to equation (48).

$$\frac{dm}{dt} = \alpha_m(1-m) - \beta_m m \quad (6)$$

$$\frac{dh}{dt} = \alpha_h(1-h) - \beta_h h \quad (7)$$

$$\alpha_m = C_{\alpha m} \frac{V_t - V_m + 25}{exp(\frac{V_t - V_m + 25}{10}) - 1} \quad \beta_m = C_{\beta m} exp(\frac{V_t - V_m}{18}) \quad (8)$$

$$\alpha_h = C_{\alpha h}.\exp(\frac{V_t - V_m}{20.0}) \beta_h = C_{\beta h} \frac{1}{\exp\left(\frac{V_t - V_m + 30}{10}\right) + 1} \quad (9)$$

Potassium channels

$$p_K = P_K n^4 + p_{K,com} \quad (10)$$

where $p_{K,com}$ due to the synaptic communication is determined according to equation (49).

$$\frac{dn}{dt} = \alpha_n(1-n) - \beta_n n \quad (11)$$

$$\alpha_n = C_{\alpha_n} \frac{V_m + 10}{\exp\left(\frac{V_m + 10}{10}\right) - 1} \quad (12)$$

$$\beta_n = C_{\beta_n} \exp(\frac{V_m}{80}) \quad (13)$$

Potassium type A

$$p_{K_A} = P_{K_A} a^3 b \quad (14)$$

$$\frac{da}{dt} = \alpha_a(1-a) - \beta_a a \quad (15)$$

$$\frac{db}{dt} = \alpha_b(1-b) - \beta_b b \quad (16)$$

$$\alpha_a = C_{\alpha_a} \frac{V_m+40}{\exp\left(\frac{V_m+40}{-15}\right)-1} \quad (17)$$

$$\beta_a = C_{\beta_a} \frac{V_m+50}{\exp\left(\frac{V_m+50}{8}\right)-1}$$

$$\alpha_b = C_{\alpha_b} \frac{1}{\exp\left(\frac{V_m-22}{15}\right)}$$

(18)

$$\beta_b = C_{\beta_b} \frac{1}{\exp\left(\frac{V_m+33}{-12}\right)+1}$$

(19)

Chloride channels

$$p_{Cl} = P_{Cl} \frac{1}{1+\exp\left(\frac{-1.28(V_m+18.1)}{-1.381\times10^{-2}}\right)} + p_{Cl,com}, \quad (20)$$

where $p_{Cl,com}$ due to the synaptic communication is determined according to equation (54).

Parameters for the permeability calculation are listed in Table 1.

TABLE 1

	Pyramidal Cell	Interneuron (Basket Cell)
Permeability constant for soma neuron	$P_{Na} = 586.0$	$P_{Na} = 524.0$
	$P_K = 60.0$	$P_K = 50.0$
	$P_{Cl} = 9.4$	$P_{Cl} = 1.4$
	$P_{Ca} = 4.2$	$P_{Ca} = 4.2$
Permeability constant pre-synaptic terminal	$P_{Ca} = 336$	$P_{Ca} = 336$

Constants for Na^+ channels	$C_{\alpha_M} = 0.25$	$C_{\alpha_M} = 0.5$
	$C_{\beta_M} = 10.0$	$C_{\beta_M} = 20.0$
	$C_{\alpha_H} = 0.075$	$C_{\alpha_H} = 0.35$
	$C_{\beta_H} = 2.5$	$C_{\beta_H} = 5.0$
Constants for K^+ channels	$C_{\alpha_N} = 0.002$	$C_{\alpha_N} = 0.005$
	$C_{\beta_N} = 0.025$	$C_{\beta_N} = 0.0625$
Constant for K^+ type A channels	$C_{\alpha_a} = -0.1$	$C_{\alpha_a} = -0.25$
	$C_{\beta_a} = 0.2$	$C_{\beta_a} = 0.5$
	$C_{\alpha_b} = 1,5.10^{-5}$	$C_{\alpha_b} = 7,5.10^{-5}$
	$C_{\beta_b} = 0.12$	$C_{\beta_b} = 0.3$
Constant for Ca^{++} channels	$C_{\alpha_c} = 0.25$	$C_{\beta_c} = 10$
	$C_{\alpha_d} = 0.075$	$C_{\beta_d} = 2.5$

Stimulation current:

$$I_{inj} = 360.M_{n,l} \text{ ,} \tag{21}$$

where $M_{n,l}$is the input matrix from datasets.

2.2. Concentration Changes

Concentrations changes were due to the following mechanisms:

Sodium Potassium Pumps

Na^+/K^+-ATPase current calculation required the introduction of a fictive ion A^+ that has a permeability P_p. The K^+ flux and the Na^+ fluxes are calculated as follows:

$$\Phi_{pump,Na} = \frac{S_{cell}}{Z_{Na}F} 3I_p \tag{22}$$

$$\Phi_{pump,K} = -\frac{S_{cell}}{Z_K F} 2I_p \tag{23}$$

where

$$I_p = 2{,}88.10^{-9} P_p \frac{F^2}{RT} V_m \frac{([A^+]_i exp(\frac{F}{RT}V_m) - [A^+]_o)}{exp(\frac{F}{RT}V_m) - 1} \tag{24}$$

and

$$P_p = 5.142857 \times 10^2 \tanh\left(\frac{V_m+60}{10}\right) + 1.5 \tag{25}$$

$$[A^+]_o = 0,0121(\frac{[Na]_o}{34,7(1+10,638[K]_o)+[Na]_o})^3(\frac{[K]i}{4,831(1+1,168[Na]_i)+[K]_i})^2 \tag{26}$$

$$[A^+]_i = (\frac{[ATP]}{[ATP]+0,175})(\frac{[Na]_i}{0,856(1+0,207[K]_i)+[Na]_i})^3.(\frac{[K]_o}{0,094(1+0,029[Na]_o)+[K]_o})^2 \tag{27}$$

Ionic Channels

Ionic channels are voltage dependent and allow transport of Na^+, K^+ and Cl^- ions through the membrane. Z_{ion} is the ion valence (Z_{Na} = 1, Z_K = 1, Z_{Cl} = −1, Z_{Ca} = 2). Voltage-gated channel fluxes were obtained by:

$$\Phi_{ion} = \frac{S_{cell}}{Z_{ion}} \frac{F}{RT} \frac{2,88.10^{-9} Z^2 P_{ion} V_m [ion]_i exp(Z_{ion} \frac{F}{RT} Vm) - [ion]_o)}{exp(Z_{ion} \frac{F}{RT} Vm) - 1} \quad , \tag{28}$$

where P_{ion} describes the ion permeability estimated by the equations (5-13).

Chloride Cotransporters and Exchangers

Cotransporters KCC and NKCC fluxes are calculated with the following equations:

$$\Phi_{KCC} = \frac{4.12\times10^{-14}([K]_i[Cl]_i - [K]_o[Cl]_o)}{(7.34+[K]_i+[K]_o)(91.02+[Cl]_i+[Cl]_o)^2} \tag{29}$$

$$\Phi_{NKCC} = \frac{-1,506.10^{-12}([Na]_o[K]_o[Cl]_o^2 - [Na]_i[K]_i[Cl]_i^2)}{(70+[Na]_i+[Na]_o)(2,3+[K]_i+[K]_o)(25,0+[Cl]_i+[Cl]_o)^2} \tag{30}$$

Exchangers

$$\Phi_{E,Na} = \frac{7,52.10^{-19}[Na]_i}{[Na]_i + 10(1+0.01[K]_i)} \tag{31}$$

$$\Phi_{E,K} = \frac{7,52.10^{-19}[K]_i}{[K]_i + 100(1+0,1[Na]_i)} \tag{32}$$

$$\Phi_{E,Cl} = \frac{4,813.10^{-19}[Cl]_i}{[Cl]_i + 6} \tag{33}$$

Electrodiffusion

Electrodiffusion (ED) was described in the model by the simultaneous effect of the electric field and the ionic concentration gradient along the extracellular

space, affecting mutually neighboring neurons. Therefore, the representation of the non-synaptic interaction in the RSNNs was performed including the ED neuronal interaction. The ED is defined by the conjoint action of chemical diffusion and the electric field that drives movement of ions in the extracellular space. The extracellular electric field can be mainly modified by the action of the ionic currents during the action potentials; therefore, the field is modified by Na^+ and K^+ currents and by the ionic distribution along the extracellular space, which can be magnified by the tortuosity of this space.

The extracellular potential changes due to the action potential currents were estimated as follows:

$$V_{extra} = \frac{-24.10^{-2} F}{exp(\frac{1}{26.10^{-16}}(Vol_{extra} - 1{,}1.10^{-13})) + 1} 16 \sum_{n=1}^{N} \frac{3{,}14.10^{-6}(\Phi_{Na} + \Phi_K)_n}{d_n} \quad (34)$$

The extracellular ionic concentration changes used to estimate the corresponding electric field were calculated by:

$$\frac{d[ion]}{dt} = \frac{D_{ion}}{10.24}\nabla^2[ion]_o + \frac{Z_{ion}FD_{ion}}{10.24RT}\nabla[ion]_o\nabla V + \frac{Z_{ion}FD_{ion}}{10.24RT}[ion]_o\nabla^2 V \quad . \quad (35)$$

Assuming the Kirchhoff law conditions for the ionic currents in the extracellular space, the extracellular field potential can be estimated:

$$\nabla V = -\frac{RT}{F}\frac{\sum_{ion} Z_{ion} D_{ion}\nabla[ion]_o}{\sum_{ions} {Z_{ion}}^2 D_{ion}[ion]_o}. \quad (29)$$

Adding to the previous equation, the field effect derived from (27) is as follows:

$$\nabla V = -\frac{RT}{F}\frac{\sum_{ion} Z_{ion} D_{ion} \nabla [ion]_o}{\sum_{ions} {Z_{ion}}^2 D_{ion} [ion]_o} + \nabla V_{extra}. \quad (36)$$

2.3. Synaptic communication

The synaptic communication between neurons was based on the work of Teixeira et al.(43). A presynaptic compartment receives an impulse from its cell body. The synaptic transmission, sensitive to the impulse, can be described in 8 steps (Figure 2.B):

• Impulse depolarizes the presynaptic terminal (Figure 2B - 1)

• The voltage dependent channels open to promote the influx of Ca^{2+}(Figure 2B - 2). Membrane depolarization altersCa^{2+} permeability.

• Intracellular Ca^{2+}increases in the presynaptic terminal, which permits exocytosis of vesicles and neurotransmitter release (Figure 2B - 3);

• Neurotransmitters, after diffusion in the synaptic cleft, bind to receptors on the postsynaptic neuron (Figure 2B - 4);

• Receptors, after neurotransmitter binding, open channels. The permeability changes for the corresponding ions create variations of membrane potential in the postsynaptic neuron in a manner dependent on the Nernst potential of the ion channel (Figure 2B - 5);

• Inactivation of the neurotransmitter is due to enzymatic action, which will return the neurotransmitter to the presynaptic compartment (Figure 2B - 6);

• Storage of the neurotransmitter is performed in vesicles (Figure 2B - 7);

• A pump removes Ca^{2+} from the presynaptic compartment (Figure 2B - 8);

Each synapse is different, and variability can be modeled by introducing a coefficient, B1, that is randomly initialized and that represents the strength of the synapse. The synaptic strength is directly linked to the quantity of neurotransmitter that binds ion channels, and it affects the amplitude of permeability variation and, thus, the amplitude of the membrane potential in the postsynaptic neuron. This coefficient is also called synaptic weight, and the synaptic weight will be affected during the learning process.

From this description the following have been implemented:

Presynaptic neuron

Ca^{2+} permeability:

$$P_{Ca} = \bar{P}_{Ca}.m^3.h \tag{37}$$

where

$$\alpha_m = \frac{C_{\alpha m}.(Vt - Vm + 25)}{exp((Vm + 25)/10) - 1} \quad \text{and} \quad \beta_m = C_{\beta m}.exp(\frac{Vt - Vm}{18.0})$$

Ca^{2+} flux:

$$\phi_{Ca,channel} = 8.10^{-9}.(\frac{F^2}{RT} Z_{Ca}^2 P_{Ca} V_m [Ca]_i \frac{exp(Z_{Ca} V_m \frac{F}{RT}) - [Ca]_o}{exp(Z_{Ca} V_m \frac{F}{RT})} - 1) \tag{38}$$

$$\Phi_{Ca,pump} = \frac{3.10^{-4}}{1 - exp(-3.10^{-3}([Ca]_i - 1.10^{-2}))} \tag{39}$$

$$\phi_{Ca,soma} = 22(8.10^{-3} - [Ca]_i) \tag{40}$$

where the Ca^{2+} concentration was estimated by

$$\frac{d[Ca]_i}{dt} = -\frac{F_{vol}}{Vol_{syn}}(\phi_{Ca,pump} + \phi_{Ca,channel} + \phi_{Ca,eq}) + \phi_{Ca,soma} \quad (41)$$

$$\frac{d[Ca]_o}{dt} = \frac{F_{vol}}{Vol_o}(\phi_{Ca,pump} + \phi_{Ca,channel} + \phi_{Ca,eq}) \quad (42)$$

Neurotransmission

$$\frac{d[NT]_i}{dt} = 10,4(-\Delta T_o + 2.10^{-3} T_v) \quad \text{(NT concentration in terminal)} \quad (43)$$

$$\frac{d[NT]_o}{dt} = 8.10^2(\Delta T_o - \Delta T_o R - \Delta T_o E) \quad \text{(NT release in synaptic cleft)} \quad (44)$$

$$\frac{dToR}{dt} = 8.10^2 \Delta T_o R \quad \text{(NT binding receptor)} \quad (45)$$

$$\frac{dT_o E}{dt} = 8.10^2(\Delta T_o E - \Delta T_o EER) \quad \text{(Enzyme inactivate NT)} \quad (46)$$

$$\frac{dTV}{dt} = 8.10^2(\Delta T_o EER - 2.10^{-3} T_v) \quad \text{(NT storage in vesicle)} \quad (47)$$

where

$$\Delta T_o = 6.10^2 [NT]_i([Ca]_i - [Ca]_o)^2 \quad (48)$$

$$\Delta T_o R = (1,5[NT]_o - 3T_o R) \quad (49)$$

$$\Delta T_o E = \frac{0,4}{1 + exp(110([NT]_i - 0,98))}[NT]_o(1 - ToE) \quad (50)$$

$$\Delta T_o EER = \frac{0,16}{1 + exp(110([NT]_i - 0,98))} T_o E \quad (51)$$

Postsynaptic neuron

Excitatory synapse:

$$\frac{dP_{Na,com}}{dt} = \sum_{n_{syn}} (B1_n w_n T_o R_n) \tag{52}$$

Inhibitory synapse:

$$\frac{dP_{K,com}}{dt} = \sum_{n_{syn}} (B1_n w_n T_o R_n) \tag{53}$$

$$\frac{dP_{Cl,com}}{dt} = \sum_{n_{syn}} (B1_n w_n T_o R_n) \tag{54}$$

2.4. Phenomenological Neuronal Model

The SNN was based on the Izhikevich model neuron(44). It has been chosen because of simplicity and its corresponding low computational cost. However, despite the simplicity, it is able to reproduce a variety of electrophysiological patterns. All simulation code presented here has been developed in Fortran90. Values chosen for a , b , c , d are close to regular spiking values, with random variation of more or less 5% of the value creating variability in the network. The model of synaptic communication between neurons is established through an α -function that gives the variations, I_{pre} , emitted from the pre-synaptic neuron:

$$\frac{dVar_z}{dt} = 16\zeta_n + \frac{-1}{\tau} Var_z \tag{55}$$

$$\frac{dVar_g}{dt} = Var_z + \frac{-1}{\tau} Var_g \tag{56}$$

$$I_{pre} = 8,2.10^{-1} Var_g \tag{57}$$

where ζ_n is the activation of the pre-synaptic neuron and $\tau = 210 * dt$. Then, the current received by the post synaptic excitatory synapse:

$$I_{post} = I_{post} + \omega_{p,q} I_{pre} \tag{58}$$

and for the inhibitory synapse:

$$I_{post} = I_{post} - \omega_{p,q} I_{pre}, \tag{59}$$

where $\omega_{p,q}$ is the synaptic weight between neurons n_p and n_q .

2.5. Networks

An example of a possible neural network generated is shown in Figure 1a.The networks are feed-forward neural networks composed of excitatory pyramidal neurons and one inhibitory interneuron, as histological analyses have shown (Figure 1). Each layer l is composed of N_l neurons, and each neuron $n_{l,i}$ creates K random connections with neurons $n_{l+j,i}$ of the next layers and $K \in [1, N_{l+1}]$. All excitatory neurons from the first layer create connections to the interneuron, which project inhibitory synapses to all other layers. All neurons of the last layer were connected to a single output neuron. Variability in the neuronal activity was introduced, randomizing the threshold of the voltage-gated channels. The biophysical range of parameters used was based on available data in the literature (46). Learning rules, detailed in the methods section, have been implemented based on direct feedback alignment and Hebbian rules. Organized in layers, the network was built with each excitatory neuron projecting to the next layers. Under external stimulation, the

first layer projects excitatory synapses to the interneuron. The interneuron sends inhibitory synapses to the rest of the network. The RSNN is schematized in Figure 1b.

2.6. Learning mechanism

In this work, we proposed a new method of learning based on DFA (47) and anti-Hebbian rules. After the period of stimulation, synaptic weights are updated. $B1$ is a randomly initialized matrix such as in the DFA method, and α_i is a scale factor to adapt the range to the type of synapse. The rules are:

If the output neuron does not spike and was expected to ($Error = 1$), then:

- all excitatory synapses where the pre-synaptic neurons have spiked are enhanced:

$$\omega_{p,q} = \omega_{p,q} + \alpha_1 B1_{p,q} \zeta_p \tag{60}$$

- all synapses that project to the interneuron are decreased if the pre-synaptic and the post-synaptic have spiked (anti-Hebbian rule):

$$\omega_{p,q} = \omega_{p,q} - \alpha_2 B1_{p,q} \zeta_p \zeta_q \tag{61}$$

- all synapses that come from interneuron are decreased if the pre-synaptic neurons have spiked:

$$\omega_{p,q} = \omega_{p,q} - \alpha_3 B1_{p,q} \zeta_p \tag{62}$$

If the output neuron had spiked and was not expected to (error=-1), then:

- all excitatory synapses are decreased if the pre-synaptic and the post-synaptic have spiked (anti-Hebbian rule):

$$\omega_{p,q} = \omega_{p,q} - \alpha_2 B1_{p,q} \zeta_p \zeta_q \tag{63}$$

- all synapses involved in inhibition are enhanced if the pre-synaptic neuron has spiked:

$$\omega_{p,q} = \omega_{p,q} + \alpha_1 B1_{p,q} \zeta_p \tag{64}$$

If the output neuron has spiked and was expected to or if it has not spiked and was not expected to ($Error = 0$), then:

- no modification is performed in the network ($\omega_{p,q} = \omega_{p,q}$)

The temporal sequence is presented in Figure 3. The data window is divided into two parts. First, a current stimulation on the input neurons with a duration of 150ms, which is in the range of stimulation for an evoked potential (48–50). In addition, then a non-stimulation period of 150 ms was left to allow the system to reach equilibrium. If the output neuron has spiked at least once during the data presentation, the output state is 1 else it is 0. At the end of each data presentation, the error, which is the difference between the wanted state (0 or 1) and the output state, is determined and synapse weights are updated. The modification of synapse weight is done with a fixed value. One epoch is the time required to apply the full dataset.

2.7. Synchrony Measurement

The synchrony measurement is conducted by the methods used by (51,52). The average value of membrane potential can be calculated:

$$\bar{V}(t) = \frac{1}{N}\sum_{n} V(t) \tag{65}$$

where variance over time is $\Delta = \langle \bar{V}(t)^2 \rangle_t - \langle \bar{V}(t) \rangle_t^2$, (66)

the variance for each neuron n is: $\Delta_n = \langle \bar{V}_n(t)^2 \rangle_t - \langle \bar{V}_n(t) \rangle_t^2$, (67)

and the synchrony is therefore $Sync = \dfrac{\Delta}{\frac{1}{N}\sum_{n} \Delta_i}$. (68)

The measure is dimensionless with a value between 0 and 1. Higher values represent more synchronism in the network.

2.8. Task

Tasks were based on an "*exclusive or"* problem (53). A cell assembly may be considered as a dynamic logical gate (54). The task has been chosen to show the ability of the computational unit (i.e., the cell assembly) to solve a nonlinear separation problem, as resumed in Table 2.

Table 2

Input	Output
0 0 0 0	0
1 1 1 1	0
1 1 0 0	1
0 0 1 1	1

To investigate the ability of our networks in solving more complex tasks, two investigations were performed. The first is the recognition of the vertical or horizontal orientation in a square of three by three. The network, with nine inputs, must separate these two classes, three rows, and three columns options. The second is to separate a pattern, the letter 'H', from a random pattern. The random pattern was generated having an input number of activated neurons with the same mean and standard deviation of the 'H' pattern.

3. Results

Networks with 5 layers and 4 neurons each have been tested on a non linear simple task (53). Our main evaluation criterion was the number of epochs required to converge (NEC; i.e., how many times the stimuli patterns set must be applied to obtain a stable correct output). We generated 1000 networks from this framework. The networks generated had a median NEC of 18, confirming the ability of the networks to converge with the proposed rules of learning.

To be more realistic, we introduced more variability in relation to the synapses and networks. To evaluate the effect of introducing variability, we first implemented variability in connectivity and then in synaptic strength. Therefore, also assuming that the neurons can randomly create synapses to neurons of the next two layers, we generated 1000 networks and observed a median NEC of 17. Following that we tested the randomly initialized synapses' strength. After generating 1000 networks, the median NEC

observed was 14. As shown in Figure 4c, the variability did not significantly change the NEC of the generated networks.

We sought to make our framework closer to biological reality. Works have shown the importance of non-synaptic mechanisms in electrophysiological activities of neurons (14,15). The non-synaptic communications occur through their influence towards their neighbors. This influence is due to ionic diffusion and variation of the electric field in the extracellular space. We refer to the interplay of these mechanisms (described in the methods) as the ED. First, we investigated the effect of the ED acting uniformly. The ED had a homogeneous effect in the network and the median NEC became higher in this case (=29). Then, we introduced variability in the ED effect, mimicking the tortuosity of the extracellular space of the neural tissue. By using this approach, the median NEC decreased to 3. In this case, the effect of the non-synaptic interconnection mediated by the ED permits fast propagation and an efficient influence for convergence.

After this observation, we sought to identify the electrophysiological activities underlying the convergence. Based on the previous simulation, we looked at the times series of the membrane potential of neurons. We observed that after convergence, some neurons presented bursting behavior and others spiking behaviors; an example is given in Figure 4 (a) and (b). The arrival of a stimulus in the network facilitates the appearance of strong activities and bursts. An increase of activity was observed before stabilization to the convergence states where spiking and bursting emerged from the morphological and functional characteristic of the network. This result is consistent with observations in experimental recording (55–57).

In this context we sought to investigate the synchrony (52,58,59). Synchrony in a neural network is strongly related to seizures and epileptiform activities (60–62). We generated 1000models with ED and variability in voltage-gated channel thresholds, synapse initialization, connectivity and tortuosity. In these simulations we measured synchrony, for which the median was 0.74. Due to the realistic representation of the networks, important characteristics for tissue adaptation have been identified: non-synaptic interactions and variety in the repertoire of electrophysiological patterns.

To verify if this feature would also emerge from a network of phenomenological spiking neurons, where spiking and bursting activities did not emerge as a network property but were induced as an intrinsic characteristic of an isolated neuron, we implemented a network with a similar architecture as previously described. The neurons were based on the model proposed by Izhikevich (44). The synaptic communication is described by an alpha-function (63).

We first investigated features of this framework with the same task as previously used. We tested, without the non-synaptic mechanism, the following conditions: only with spiking neurons and only with bursting neurons. Then, we introduced mechanisms of non-synaptic influences. An active neuron facilitates direct neighbors, from the same and the next layer, to produce a burst. In this condition, there appeared a mix of patterns from spikes to burst. Finally, to verify that this variety of neural behavior must be structured by the non-synaptic interactions, we generated networks with randomly initialized neurons intrinsically producing spikes or bursts.

Simulations in a condition with only spiking neurons are presented in Figure 5.a. Spikes occur sparingly and have a short duration. Due to the propagation dynamic in the network, when the last neurons activate, the first neurons are no longer active. This process explains the low values of synchrony observed. In this condition, networks needed on average more than 15 epochs to converge in the range of synchrony between 0.08 and 0.18, and the NEC becomes higher for other ranges of synchrony.

Results of simulations in conditions with only bursting neurons are presented in Figure 5.b. Bursting activity may involve higher synaptic communication (12) or higher non-synaptic interactions (14) or both. These conditions imply a high level of activity and mutual coupling in the network and, therefore, higher synchrony. The average NEC is 34, and the level of synchrony is higher than 0.7. The high level of activities and synchrony impedes convergences.

Simulations in which the activity of each neuron influences the surrounding neurons are shown in Figure 5C. In these simulations the networks resemble the non-synaptic mechanisms of the RSNN, and, therefore, control the neuronal activity for spiking or bursting. The convergence for all simulations is mainly concentrated below the dashed line, indicating less than the 20 NEC. With a synchrony between 0.5 and 0.75, networks needed, on average, fewer than 7 epochs to converge. The median NEC observed is comparable to the median NEC obtained in the RSNN (Figure 5.e). This condition presents its best configurations for fast convergence and is biologically more plausible and closest to the RSNN.

To confirm that the mix of bursts and spikes must come up as an emerging property of the network to increase convergence, we tested a condition with random initialization of spiking and bursting neurons in the network. Then, each neuron will only produce one of these behaviors during the simulation. In this case, the majority of the simulations have a maximal value of synchrony in the same range as found with networks of bursting neurons (>0.7) (Figure 5.d), and the average NEC was 38. Because each neuron is initialized randomly, it produces an activity, which may not be in accordance with the network configuration. As networks connections are also randomly initialized, the adaptive process to find paths for convergence is difficult.

Testing the ability of our networks to be applied for more complex machine learning tasks, we performed two additional studies. The first study is based on orientation detection, as shown in Figure 6 (a) - left. Two thousand networks were generated to perform the task, and two groups were taken into account: one thousand networks including non-synaptic interactions and one thousand networks with only synaptic communication. Each network was composed of 5 layers of 9 neurons. In Figure 6 (a) - left, we present a histogram of the number of epochs required to obtain a complete separation (i.e., with no error) of our two datasets (vertical and horizontal), which is presented in red for the group of networks taking into account non-synaptic influences and in blue for the group of networks with only synaptic communication. We observed that networks taking into account non-synaptic interactions are, on average, faster to solve such tasks. Correspondently for each group, in Figure 6(a) – right, we show a histogram of the proportion of

networks in the corresponding interval of levels of synchronism. This panel highlights that the group of the networks with non-synaptic influences are more frequent in higher synchronism.

The second study is based on the separation of two classes: handwritten 0 and 1 extracted from the UCI repository (64), and the available dataset used is given in (65). The 8×8 images used for this task are presented in Figure 6b.One hundred synaptic networks made of 8 layers of 64 neurons were generated to perform this task. The other one hundred networks taking into account non-synaptic interactions were generated to perform the same task. For both cases, we measured the error rate as the normalized number of wrong classifications per epoch. The results are presented in Figure 6 (b) - left and show that networks taking into account non-synaptic interactions produced less than 10% of the error after 5 epochs, whereas almost twice the number of epochs are required by only synaptic networks. These two studies offer an overview of the potential of the networks taking into account non-synaptic interactions for fast learning in a spiking neural network for machine learning applications. It is also evident there was an increased level of synchronism of the group of networks including the non-synaptic interactions Figure 6(b) - right.

4. Discussion

In this work, we first showed the importance of non-synaptic interactions in a small cell assembly due to a detailed biophysical model. The non-synaptic influence of neurons to neighbors occurs mainly due to ED. The

ED has been demonstrated to have a strong effect between neurons in the neural tissue (66) and may be a factor for pathological states(14,45,67,68).This finding could be explained by the fact that the ED modulates neuronal excitability and, thus, the type of electrophysiological pattern. However, if all neighboring neurons of the cell assemblies receive the same influence from ED, the ability of the cell assembly to quickly process information vanished.

This situation does not exist in the brain, as it is not homogeneous but is,in fact, a tortuous tissue(69,70). In our model, the introduction of tortuosity facilitates the emergence of a specific propagation path for each stimulus and, thus, makes the system converge even faster. The complex local anatomy of the brain would therefore be one of the causes of its efficiency in processing information. The information propagates through neural activation. Neural activities have often been considered as binary, with a resting state and a punctual spike. However, spikes in biological systems are not the only discrete events, but they do constitute one of the patterns observed in the large repertoires of the electrophysiological behavior of neuron membranes. Burst activities are important for information transmission (12,71) but also participate in neural synchrony in epilepsy (72). We observed that a mix of pattern activities (bursting and spiking) is the most efficient but only when the pattern depends on neighborhood influences. With random parameterization of neurons to produce spikes or bursts, convergence is difficult, as it limits the emergence of structured paths.

This was verified in a phenomenological model, reproducing behavior observed in the biophysical model. In this second model, the implantation of non-synaptic interactions between neurons also promoted fast convergence in the networks. As it had a low computational cost, the simplified model is a good candidate for building networks of interacting cell assemblies, as is the modeling of larger regions of the brain, which takes into account the variety of electrophysiological patterns.

Strong and synchronous activities may lead to pathological states, such as seizures. We measured the synchrony in the generated network and investigated if it was related to the ability to fast converge. We generated numerous models and observed that networks with a low NEC presented an increased level of synchrony, following what was observed for the RSMM. According to previous findings (20), we also observed different configurations can converge for the same task. The generated models of the network might converge at different speeds with different levels of synchrony. This finding explains the inter individual differences both in the ability to process information and the potential for entering pathological states. Some cell assemblies are more likely to trigger seizures than others. This finding may explain why between individuals able to process information in the same way there is an inequality of the probability of triggering epileptic episodes. Cell assemblies work efficiently and produce a high range of synchrony; so, cell assemblies are not far to promote epilepsy.

Synchrony in the brain is observed in the hippocampus, participating in neurodevelopment and memory formation (73,74). It is a marker of intense

neural activities. Throughout history, many important personalities, such as Socrates, Hermann von Helmholtz, Alfred Nobel, Vincent Van Gogh, Molière, Gustave Flaubert, Fiodor Dostoïevski, Edgar Allan Poe, Charles Dickens, Joaquim Maria Machado de Assis, and Pyotr Ilyich Tchaikovsky, all lived with epilepsy. They all distinguished themselves in history by a high creative potential. Epilepsy and creativity have been often related (75,76). Why would epilepsy be correlated with creativity? If causality exists, why do not all people with epilepsy present with higher creative faculties?

At the cell assembly scale, our current work gives new insight into this question. The ability to rapidly treat and correlate various information may lead to unusual semantic associations, and so facilitate creative thinking (77). Some morphologic configurations of networks that promote creativity may also lead to seizures and may be identified as one more tributary of the river of epilepsy (78). This fact may also explain why epilepsy is not always associated with creativity (79). Some of tributaries are not related to creativity networks (78). This hypothesis is consistent with the effects of anti-epileptic drugs. By reducing neural activity synchrony (80), drugs may also produce side effects on mental activities (81) and on creativity (82).

Our work provides some insights into the underlying mechanisms of epileptogenesis on the scale of cell assembly. During neurogenesis, the neural tissue can be organized with high variability, leading to numerous possible configurations. Cell assemblies work with a high level of synchrony. A few configurations may facilitate crossing the limit between the healthy and efficient synchrony to seizures.

The relationship between neuroscience and machine learning may in essence have different goals. Neurosciences aim to understand brain mechanisms, while machine learning works toward functional optimization (42). In this work, we proposed observations from a neuroscience point of view about learning, which may have implications for machine learning applications. Our detailed biophysical model permits a fine understanding of biophysical mechanisms and their relation to emergent properties in the network. This model implies a very high computational cost; as such, it does not offer, in its complete version, a solution for machine learning applications. However, it should be considered as a tool to determine which mechanisms are relevant for learning.

Due to this method, we identified two important components that can be reproduced in a simplified network, offering new direction for the development of spiking neural networks. First, we showed the importance of two levels of interactions (synaptic and non-synaptic) between neurons for efficient learning. This finding supports the idea of the existence of two networks at different temporal and spatial scales: a conventional synaptic network and a local (non-synaptic) network acting on different intrinsic properties of each neuron in the cell assembly. Actual tools to build large spiking neural networks(83) are not currently viable, although such tools might be plausible in the near future. The second component is related to the pattern of neuronal activity (i.e., single peak or burst). The selection of the pattern of neuronal activity is easy to implement, as it only depends on the model chosen to produce the spiking or busting activity. In line with this finding, a recent work, based on integrate-and-fire models, confirmed the

importance of bursting to increase the efficiency of the network for machine learning applications (84).

5. Conclusion

In this work, we proposed models of cell assemblies as building blocks for PDP. First, we proposed biologically plausible mechanisms of synaptic weight adaptation. We show the ability of this rule to provide learning in biophysical models of cell assemblies. In this biophysical framework, we identified important properties that influence the network convergence: the effect of ED and variability in the tissue. We showed that a network including two levels of interaction, with different temporal and spatial scales, might be more efficient for fast convergence. The two levels of interaction are: the local level, through non-synaptic interactions, and the larger level, through synaptic communication. We implemented a network based on phenomenological descriptions taking into account these previous observations. Then, we showed a strong relationship between the level of synchrony and the ability of the cell assembly to quickly process information. The high level of synchrony observed during fast processing may suggest that to be efficient cell assemblies must work close to the threshold of seizure. The two levels of interaction show another possible way connections between neurons might be created to promote deep learning. The synchronism induced and sustained by this network structure represents deep knowledge and enables the brain to more efficiently perform complex tasks, such as pattern recognition. On the other hand, the improper improvement of these kinds of connections might

enhance the synchronism (hypersynchronism) in an inconvenient manner, thus spreading to the whole network and leading to functional states that synchronism and hypersynchronism domains, when deep learning may or may not be performed, respectively.

Acknowledgments

This work was supported by the Brazilian agencies Fundação de Amparo à Pesquisa de Minas Gerais (FAPEMIG), Fundação de Amparo à Pesquisa do Estado de São Paulo (FAPESP), Conselho Nacional de Desenvolvimento Científico e Tecnológico (CNPq), Programa Nacional de Cooperação Acadêmica/ Coordenação de Aperfeiçoamento de Pessoal de Nível Superior (PROCAD/CAPES) and Instituto Nacional de Neurociência Translacional (INNT) of Translational Neuroscience (Ministério da Ciência e Tecnologia/CNPq/FAPESP).

References

1. Hebb DO. The Organization of Behavior; A Neuropsychological Theory. Am J Psychol [Internet]. 1950 [cited 2019 Jan 21];63(4):633. Available from: http://lib1.org/_ads/137FE4452E446B1851177F4145320724

2. Shaw GL, Harth E, Scheibel AB. Cooperativity in brain function: Assemblies of approximately 30 neurons. Exp Neurol [Internet]. 1982 Aug 1 [cited 2019 Feb 10];77(2):324–58. Available from: https://www.sciencedirect.com/science/article/pii/0014488682902497

3. Rumelhart DE, McClelland JL. Parallel distributed processing : explorations in the microstructure of cognition. University of California SDPRG, editor. MIT Press; 1986.

4. Setareh H, Deger M, Gerstner W. Excitable neuronal assemblies with adaptation as a building block of brain circuits for velocity-controlled signal propagation. van Rossum MCW, editor. PLOS Comput Biol [Internet]. 2018 Jul 6 [cited 2019 Jan 30];14(7):e1006216. Available from: https://dx.plos.org/10.1371/journal.pcbi.1006216

5. Poirazi P, Brannon T, Mel BW. Pyramidal Neuron as Two-Layer Neural Network. Neuron [Internet]. 2003 Mar 27 [cited 2019 Jan 24];37(6):989–99. Available from: https://www.sciencedirect.com/science/article/pii/S0896627303001491

6. Laughlin SB, Sejnowski TJ. Communication in neuronal networks. Science [Internet]. 2003 Sep 26 [cited 2019 Jan 24];301(5641):1870–4. Available from: http://www.ncbi.nlm.nih.gov/pubmed/14512617

7. Wang X. Neural coding strategies in auditory cortex. Hear Res [Internet]. 2007 Jul 1 [cited 2019 Feb 1];229(1–2):81–93. Available from: https://www.sciencedirect.com/science/article/pii/S0378595507000366

8. Ostwald D, Lam JM, Li S, Kourtzi Z. Neural Coding of Global Form in the Human Visual Cortex. J Neurophysiol [Internet]. 2008 May [cited 2019 Feb 1];99(5):2456–69. Available from: http://www.physiology.org/doi/10.1152/jn.01307.2007

9. Eichenbaum H. The hippocampus and declarative memory: cognitive mechanisms and neural codes. Behav Brain Res [Internet]. 2001 Dec

14 [cited 2019 Feb 1];127(1–2):199–207. Available from: https://www.sciencedirect.com/science/article/pii/S0166432801003655

10. Deco G, Buehlmann A, Masquelier T, Hugues E. The role of rhythmic neural synchronization in rest and task conditions. Front Hum Neurosci [Internet]. 2011 [cited 2019 Sep 12];5:4. Available from: http://www.ncbi.nlm.nih.gov/pubmed/21326617

11. Cessac B, Paugam-Moisy H, Viéville T. Overview of facts and issues about neural coding by spikes. J Physiol [Internet]. 2010 Jan [cited 2019 Jan 21];104(1–2):5–18. Available from: http://www.ncbi.nlm.nih.gov/pubmed/19925865

12. Lisman J. Bursts as a unit of neural information: making unreliable synapses reliable. Trends Neurosci [Internet]. 1997 Jan [cited 2019 Jan 21];20(1):38–43. Available from: http://www.ncbi.nlm.nih.gov/pubmed/9004418

13. Zeldenrust F, Chameau PJP, Wadman WJ. Reliability of spike and burst firing in thalamocortical relay cells. J Comput Neurosci [Internet]. 2013 Dec 25 [cited 2019 Jan 21];35(3):317–34. Available from: http://www.ncbi.nlm.nih.gov/pubmed/23708878

14. de Almeida A-CG, Rodrigues AM, Scorza FA, Cavalheiro EA, Teixeira HZ, Duarte MA, et al. Mechanistic hypotheses for nonsynaptic epileptiform activity induction and its transition from the interictal to ictal state-Computational simulation. Epilepsia [Internet]. 2008 Nov [cited 2019 Jan 12];49(11):1908–24. Available from: http://www.ncbi.nlm.nih.gov/pubmed/18513350

15. Jefferys JG, Haas HL. Synchronized bursting of CA1 hippocampal pyramidal cells in the absence of synaptic transmission. Nature [Internet]. 1982 Dec 2 [cited 2019 Jan 13];300(5891):448–50. Available from: http://www.ncbi.nlm.nih.gov/pubmed/6292731

16. Poo M-M, Pignatelli M, Ryan TJ, Tonegawa S, Bonhoeffer T, Martin KC, et al. What is memory? The present state of the engram. BMC Biol [Internet]. 2016 [cited 2019 Feb 12];14:40. Available from: http://www.ncbi.nlm.nih.gov/pubmed/27197636

17. Benjamin PR, Kemenes G, Kemenes I. Non-synaptic neuronal mechanisms of learning and memory in gastropod molluscs. Front Biosci [Internet]. 2008 May 1 [cited 2019 Feb 1];13:4051–7. Available from: http://www.ncbi.nlm.nih.gov/pubmed/18508499

18. Nikitin ES, Balaban PM, Kemenes G. Nonsynaptic Plasticity Underlies a Compartmentalized Increase in Synaptic Efficacy after Classical Conditioning. Curr Biol [Internet]. 2013 Apr [cited 2019 Feb 1];23(7):614–9. Available from: https://linkinghub.elsevier.com/retrieve/pii/S0960982213002558

19. Mozzachiodi R, Byrne JH. More than synaptic plasticity: role of nonsynaptic plasticity in learning and memory. Trends Neurosci [Internet]. 2010 Jan [cited 2019 Feb 1];33(1):17–26. Available from: http://www.ncbi.nlm.nih.gov/pubmed/19889466

20. Prinz AA, Bucher D, Marder E. Similar network activity from disparate circuit parameters. Nat Neurosci [Internet]. 2004 Dec 21 [cited 2019 Jan 13];7(12):1345–52. Available from:

http://www.nature.com/articles/nn1352

21. Howard MW, Eichenbaum H. The hippocampus, time, and memory across scales. J Exp Psychol Gen [Internet]. 2013 Nov [cited 2019 Feb 1];142(4):1211–30. Available from: http://www.ncbi.nlm.nih.gov/pubmed/23915126

22. Knierim JJ. The hippocampus. Curr Biol [Internet]. 2015 Dec 7 [cited 2019 Feb 1];25(23):R1116–21. Available from: https://www.sciencedirect.com/science/article/pii/S0960982215013123

23. Sweatt JD. Hippocampal function in cognition. Psychopharmacology (Berl) [Internet]. 2004 Jun 2 [cited 2019 Feb 16];174(1):99–110. Available from: http://link.springer.com/10.1007/s00213-004-1795-9

24. Holmes GL. Cognitive impairment in epilepsy: the role of network abnormalities. Epileptic Disord [Internet]. 2015 Jun [cited 2019 Feb 16];17(2):101–16. Available from: http://www.ncbi.nlm.nih.gov/pubmed/25905906

25. Dragoi G, Buzsáki G. Temporal Encoding of Place Sequences by Hippocampal Cell Assemblies. Neuron [Internet]. 2006 Apr 6 [cited 2019 Jan 21];50(1):145–57. Available from: http://www.ncbi.nlm.nih.gov/pubmed/16600862

26. Harris KD, Csicsvari J, Hirase H, Dragoi G, Buzsáki G. Organization of cell assemblies in the hippocampus. Nature [Internet]. 2003 Jul 31 [cited 2019 Jan 21];424(6948):552–6. Available from: http://www.ncbi.nlm.nih.gov/pubmed/12891358

27. Snow RW, Taylor CP, Dudek FE. Electrophysiological and optical changes in slices of rat hippocampus during spreading depression. J Neurophysiol [Internet]. 1983 Sep [cited 2019 Feb 1];50(3):561–72. Available from: http://www.ncbi.nlm.nih.gov/pubmed/6311993

28. Lietsche J, Imran I, Klein J. Extracellular levels of ATP and acetylcholine during lithium-pilocarpine induced status epilepticus in rats. Neurosci Lett [Internet]. 2016 Jan 12 [cited 2019 Jan 13];611:69–73. Available from: http://www.ncbi.nlm.nih.gov/pubmed/26610905

29. Bikson M, Hahn PJ, Fox JE, Jefferys JGR. Depolarization Block of Neurons During Maintenance of Electrographic Seizures. J Neurophysiol [Internet]. 2003 Oct [cited 2019 Jan 12];90(4):2402–8. Available from: http://www.ncbi.nlm.nih.gov/pubmed/12801897

30. Cressman JR, Ullah G, Ziburkus J, Schiff SJ, Barreto E. The influence of sodium and potassium dynamics on excitability, seizures, and the stability of persistent states: I. Single neuron dynamics. J Comput Neurosci [Internet]. 2009 Apr 24 [cited 2019 Jan 12];26(2):159–70. Available from: http://www.ncbi.nlm.nih.gov/pubmed/19169801

31. Lieb JP, Walsh GO, Babb TL, Walter RD, Crandall PH, Tassinari CA, et al. A Comparison of EEG Seizure Patterns Recorded with Surface and Depth Electrodes in Patients with Temporal Lobe Epilepsy. Epilepsia [Internet]. 1976 Jun 1 [cited 2019 Feb 12];17(2):137–60. Available from: http://doi.wiley.com/10.1111/j.1528-1157.1976.tb03392.x

32. Jenssen S, Roberts CM, Gracely EJ, Dlugos DJ, Sperling MR. Focal seizure propagation in the intracranial EEG. Epilepsy Res [Internet].

2011 Jan [cited 2019 Feb 12];93(1):25–32. Available from: http://www.ncbi.nlm.nih.gov/pubmed/21130604

33. Queenan BN, Pak DT. Homeostatic synaptic plasticity in the hippocampus: Therapeutic prospects for seizure control? Future Neurol. 2013;8(4):361–3.

34. Scharfman HE. Epilepsy as an example of neural plasticity. Neuroscientist [Internet]. 2002 Apr [cited 2019 Jan 25];8(2):154–73. Available from: http://www.ncbi.nlm.nih.gov/pubmed/11954560

35. Kleen JK, Scott RC, Holmes GL, Lenck-Santini PP. Hippocampal interictal spikes disrupt cognition in rats. Ann Neurol [Internet]. 2010 Feb [cited 2019 Feb 16];67(2):250–7. Available from: http://www.ncbi.nlm.nih.gov/pubmed/20225290

36. McCulloch WS, Pitts W. A logical calculus of the ideas immanent in nervous activity. Bull Math Biophys. 1943;5:115–33.

37. Rosenblatt F. The perceptron: A probabilistic model for information storage and organization in the brain. Psychol Rev [Internet]. 1958 [cited 2019 Feb 18];65(6):386–408. Available from: http://doi.apa.org/getdoi.cfm?doi=10.1037/h0042519

38. Diehl PU, Neil D, Binas J, Cook M, Liu S-C, Pfeiffer M. Fast-classifying, high-accuracy spiking deep networks through weight and threshold balancing. In: 2015 International Joint Conference on Neural Networks (IJCNN) [Internet]. IEEE; 2015 [cited 2019 May 10]. p. 1–8. Available from: http://ieeexplore.ieee.org/document/7280696/

39. Hopkins M, Pineda-García G, Bogdan PA, Furber SB. Spiking neural networks for computer vision. Interface Focus [Internet]. 2018 Aug 6 [cited 2019 May 10];8(4):20180007. Available from: http://www.ncbi.nlm.nih.gov/pubmed/29951187

40. Kasabov NK. Time-Space , Spiking Neural Networks and Brain-Inspired Artificial Intelligence. Springer; 2019.

41. Carrillo-Medina JL, Latorre R. Implementing Signature Neural Networks with Spiking Neurons. Front Comput Neurosci [Internet]. 2016 [cited 2019 May 10];10:132. Available from: http://www.ncbi.nlm.nih.gov/pubmed/28066221

42. Marblestone AH, Wayne G, Kording KP. Toward an Integration of Deep Learning and Neuroscience. Front Comput Neurosci [Internet]. 2016 Sep 14 [cited 2019 May 9];10:94. Available from: http://journal.frontiersin.org/Article/10.3389/fncom.2016.00094/abstract

43. Teixeira HZ, Almeida A-CG, Infantosi AFC, Rodrigues AM, Costa NL, Duarte MA. Identifying essential conditions for refractoriness of Leão's spreading depression—Computational modeling. Comput Biol Chem [Internet]. 2008 Aug 1 [cited 2019 Jan 24];32(4):273–81. Available from: https://www.sciencedirect.com/science/article/pii/S1476927108000406

44. Izhikevich EM. Simple model of spiking neurons. IEEE Trans Neural Networks [Internet]. 2003 Nov [cited 2019 Jan 24];14(6):1569–72. Available from: http://www.ncbi.nlm.nih.gov/pubmed/18244602

45. Rodrigues AM, Santos LEC, Covolan L, Hamani C, Almeida A-CG. pH during non-synaptic epileptiform activity—computational simulations.

Phys Biol [Internet]. 2015 Sep 2 [cited 2019 Feb 17];12(5):056007. Available from: http://stacks.iop.org/1478-3975/12/i=5/a=056007?key=crossref.0f726d82c5beae730f8610871d033b8e

46. Wheeler DW, White CM, Rees CL, Komendantov AO, Hamilton DJ, Ascoli GA. Hippocampome.org: a knowledge base of neuron types in the rodent hippocampus. Elife [Internet]. 2015 Sep 24 [cited 2019 Jan 26];4. Available from: https://elifesciences.org/articles/09960

47. Nokland A. Direct Feedback Alignment Provides Learning in Deep Neural Networks [Internet]. 2016 [cited 2019 Feb 4]. Available from: https://www.semanticscholar.org/paper/Direct-Feedback-Alignment-Provides-Learning-in-Deep-Nokland/6fd7ba8549887eea247f674d30845ee03d0a530c

48. Fujii M, Yamada T, Aihara M, Kokubun Y, Noguchi Y, Matsubara M, et al. The effects of stimulus rates upon median, ulnar and radial nerve somatosensory evoked potentials. Electroencephalogr Clin Neurophysiol [Internet]. 1994 Nov [cited 2019 Feb 10];92(6):518–26. Available from: http://www.ncbi.nlm.nih.gov/pubmed/7527770

49. Manganotti P, Storti SF, Formaggio E, Acler M, Zoccatelli G, Pizzini FB, et al. Effect of median-nerve electrical stimulation on BOLD activity in acute ischemic stroke patients. Clin Neurophysiol [Internet]. 2012 Jan [cited 2019 Feb 10];123(1):142–53. Available from: http://www.ncbi.nlm.nih.gov/pubmed/21741301

50. Van Dun B, Carter L, Dillon H. Sensitivity of cortical auditory evoked

potential detection for hearing-impaired infants in response to short speech sounds. Audiol Res [Internet]. 2012 Jan 9 [cited 2019 Feb 10];2(1):e13. Available from: http://www.ncbi.nlm.nih.gov/pubmed/26557328

51. Golomb D, Rinzel J. Dynamics of globally coupled inhibitory neurons with heterogeneity. Phys Rev E [Internet]. 1993 Dec 1 [cited 2019 Feb 17];48(6):4810–4. Available from: https://link.aps.org/doi/10.1103/PhysRevE.48.4810

52. Uzuntarla M, Barreto E, Torres JJ. Inverse stochastic resonance in networks of spiking neurons. PLOS Comput Biol [Internet]. 2017;13(7):e1005646. Available from: http://dx.plos.org/10.1371/journal.pcbi.1005646

53. Reljan-Delaney M, Wall J. Solving the linearly inseparable XOR problem with spiking neural networks. In: 2017 Computing Conference [Internet]. IEEE; 2017 [cited 2019 Jan 21]. p. 701–5. Available from: http://ieeexplore.ieee.org/document/8252173/

54. Goldental A, Guberman S, Vardi R, Kanter I. A computational paradigm for dynamic logic-gates in neuronal activity. Front Comput Neurosci [Internet]. 2014 [cited 2019 Feb 20];8:52. Available from: http://www.ncbi.nlm.nih.gov/pubmed/24808856

55. Starosta S, Stüttgen MC, Güntürkün O. Recording single neurons' action potentials from freely moving pigeons across three stages of learning. J Vis Exp [Internet]. 2014 Jun 2 [cited 2019 Jan 24];(88). Available from: http://www.ncbi.nlm.nih.gov/pubmed/24961391

56. Lundqvist M, Rose J, Herman P, Brincat SL, Buschman TJ, Miller EK. Gamma and Beta Bursts Underlie Working Memory. Neuron [Internet]. 2016 Apr 6 [cited 2019 Jan 24];90(1):152–64. Available from: http://www.ncbi.nlm.nih.gov/pubmed/26996084

57. Sandler AJ. Chronic Recording During Learning [Internet]. Methods for Neural Ensemble Recordings. CRC Press/Taylor & Francis; 2008 [cited 2019 Jan 24]. Available from: http://www.ncbi.nlm.nih.gov/pubmed/21204449

58. Neltner L, Hansel D, Mato G, Meunier C. Synchrony in Heterogeneous Networks of Spiking Neurons. Neural Comput [Internet]. 2000 Jul 13 [cited 2019 Jan 25];12(7):1607–41. Available from: http://www.mitpressjournals.org/doi/10.1162/089976600300015286

59. Li C, Zheng Q. Synchronization of the small-world neuronal network with unreliable synapses. Phys Biol [Internet]. 2010 Sep 20 [cited 2019 Jan 25];7(3):036010. Available from: http://stacks.iop.org/1478-3975/7/i=3/a=036010?key=crossref.5c28bfdc88fdd6587d98e32905c513e4

60. Dominguez, LG. Enhanced Synchrony in Epileptiform Activity? Local versus Distant Phase Synchronization in Generalized Seizures. J Neurosci [Internet]. 2005;25(35):8077–84. Available from: http://www.jneurosci.org/cgi/doi/10.1523/JNEUROSCI.1046-05.2005

61. Jiruska P, Csicsvari J, Powell AD, Fox JE, Chang WC, Vreugdenhil M, et al. High-Frequency Network Activity, Global Increase in Neuronal Activity, and Synchrony Expansion Precede Epileptic Seizures In Vitro.

J Neurosci [Internet]. 2010;30(16):5690–701. Available from: http://www.jneurosci.org/cgi/doi/10.1523/JNEUROSCI.0535-10.2010

62. Percha B, Dzakpasu R, Żochowski M, Parent J. Transition from local to global phase synchrony in small world neural network and its possible implications for epilepsy. Phys Rev E [Internet]. 2005 Sep 16 [cited 2019 Jan 14];72(3):031909. Available from: http://www.ncbi.nlm.nih.gov/pubmed/16241484

63. Ermentrout B, Terman DH (David H. Mathematical foundations of neuroscience [Internet]. Springer; 2010 [cited 2019 Jan 24]. 422 p. Available from: http://mirror1.booksdescr.org/ads.php?md5=8C0F9776F51DC564E7FF318425350F1D

64. Dheeru D, Karra Taniskidou E. {UCI} Machine Learning Repository [Internet]. 2017. Available from: http://archive.ics.uci.edu/ml

65. Tang EK, Suganthan PN, Yao X, Qin AK. Linear dimensionality reduction using relevance weighted LDA. Pattern Recognit [Internet]. 2005 Apr 1 [cited 2019 Sep 11];38(4):485–93. Available from: https://www.sciencedirect.com/science/article/abs/pii/S0031320304003619

66. Halnes G, Mäki-Marttunen T, Keller D, Pettersen KH, Andreassen OA, Einevoll GT. Effect of Ionic Diffusion on Extracellular Potentials in Neural Tissue. PLoS Comput Biol [Internet]. 2016 Nov [cited 2019 Feb 15];12(11):e1005193. Available from: http://www.ncbi.nlm.nih.gov/pubmed/27820827

67. Nogueira GS, Santos LEC, Rodrigues AM, Scorza CA, Scorza FA, Cavalheiro EA, et al. Enhanced nonsynaptic epileptiform activity in the dentate gyrus after kainate-induced status epilepticus. Neuroscience [Internet]. 2015 Sep 10 [cited 2019 Sep 17];303:59–72. Available from: http://www.ncbi.nlm.nih.gov/pubmed/26141843

68. Amorim BO, Covolan L, Ferreira E, Brito JG, Nunes DP, de Morais DG, et al. Deep brain stimulation induces antiapoptotic and anti-inflammatory effects in epileptic rats. J Neuroinflammation [Internet]. 2015 Dec 4 [cited 2019 Sep 17];12(1):162. Available from: http://www.jneuroinflammation.com/content/12/1/162

69. Hrabětová S, Nicholson C. Contribution of dead-space microdomains to tortuosity of brain extracellular space. Neurochem Int [Internet]. 2004 Sep 1 [cited 2019 Mar 1];45(4):467–77. Available from: https://www.sciencedirect.com/science/article/abs/pii/S0197018603002511

70. Syková E, Nicholson C. Diffusion in Brain Extracellular Space. Physiol Rev [Internet]. 2008 Oct [cited 2019 Sep 17];88(4):1277–340. Available from: http://www.ncbi.nlm.nih.gov/pubmed/18923183

71. Zeldenrust F, Wadman WJ, Englitz B. Neural Coding With Bursts—Current State and Future Perspectives. Front Comput Neurosci [Internet]. 2018 Jul 6 [cited 2019 Jan 21];12:48. Available from: https://www.frontiersin.org/article/10.3389/fncom.2018.00048/full

72. Wong RK, Traub RD, Miles R. Cellular basis of neuronal synchrony in epilepsy. Adv Neurol [Internet]. 1986 [cited 2019 Feb 4];44:583–92.

Available from: http://www.ncbi.nlm.nih.gov/pubmed/3706021

73. Bonifazi P, Goldin M, Picardo MA, Jorquera I, Cattani A, Bianconi G, et al. GABAergic hub neurons orchestrate synchrony in developing hippocampal networks. Science [Internet]. 2009 Dec 4 [cited 2019 Feb 19];326(5958):1419–24. Available from: http://www.ncbi.nlm.nih.gov/pubmed/19965761

74. Buzsáki G, Bragin A, Chrobak JJ, Nádasdy Z, Sik A, Hsu M, et al. Oscillatory and Intermittent Synchrony in the Hippocampus: Relevance to Memory Trace Formation. In 1994 [cited 2019 Feb 19]. p. 145–72. Available from: http://www.springerlink.com/index/10.1007/978-3-642-85148-3_9

75. Stirling J. Representing epilepsy : myth and matter [Internet]. Liverpool University Press; 2010 [cited 2019 Feb 20]. 266 p. Available from: https://books.google.com.br/books?hl=fr&lr=&id=6xDLB1YkzJYC&oi=fnd&pg=PR7&dq=epilepsy+and+creativity&ots=erFxi1OThi&sig=pM3ULUz9Kp5CQ0oyGo3oVpTLiXI#v=onepage&q=epilepsy and creativity&f=false

76. Ronald Bradley R. Adron Harris Peter Jenner. International Review of Neurobiology: The Neurobiology of Painting [Internet]. Elsevier Academic Press; 2006. 360 p. Available from: https://www.sciencedirect.com/bookseries/international-review-of-neurobiology/vol/74

77. Eysenck HJ. Genius [Internet]. Cambridge: Cambridge University Press; 1995 [cited 2019 Feb 20]. Available from:

http://ebooks.cambridge.org/ref/id/CBO9780511752247

78. Lytton WW. Computer modelling of epilepsy. Nat Rev Neurosci [Internet]. 2008 Aug [cited 2019 Jan 23];9(8):626–37. Available from: http://www.ncbi.nlm.nih.gov/pubmed/18594562

79. Cartwright M, Clark-Carter D, Ellis SJ, Matthews C. Temporal Lobe Epilepsy and Creativity: A Model of Association. Creat Res J [Internet]. 2004 Mar [cited 2019 Feb 20];16(1):27–34. Available from: http://www.tandfonline.com/doi/abs/10.1207/s15326934crj1601_3

80. Nayak CS, Mariyappa N, Majumdar KK, Ravi GS, Prasad PD, Nagappa M, et al. NREM Sleep and Antiepileptic Medications Modulate Epileptiform Activity by Altering Cortical Synchrony. Clin EEG Neurosci [Internet]. 2018 Nov 8 [cited 2019 Feb 20];49(6):417–24. Available from: http://www.ncbi.nlm.nih.gov/pubmed/29308656

81. Reynolds EH. Mental Effects of Antiepileptic Medication: A Review. Epilepsia [Internet]. 1983 Oct [cited 2019 Feb 20];24(s2):S85–95. Available from: http://doi.wiley.com/10.1111/j.1528-1157.1983.tb04651.x

82. Zubkov S, Friedman D. Epilepsy treatment and creativity. Epilepsy Behav [Internet]. 2016 Apr 1 [cited 2019 Feb 20];57:230–3. Available from: https://www.sciencedirect.com/science/article/pii/S1525505016000044

83. Hazan H, Saunders DJ, Khan H, Patel D, Sanghavi DT, Siegelmann HT, et al. BindsNET: A Machine Learning-Oriented Spiking Neural Networks Library in Python. Front Neuroinform [Internet]. 2018 Dec 12

[cited 2019 May 9];12:89. Available from:

https://www.frontiersin.org/article/10.3389/fninf.2018.00089/full

84. Park S, Kim S, Choe H, Yoon S. Fast and Efficient Information Transmission with Burst Spikes in Deep Spiking Neural Networks. 2018 Sep 10 [cited 2019 May 9]; Available from:

http://arxiv.org/abs/1809.03142

LEGENDS

Figure 1. Scheme of a realistic spiking neural network. **(a)** Confocal micrograph of a hippocampal slice stained to distinguish neurons and interneurons. **(b)** Representative drawing of the picture shown in (a), based on which the RSNN **(c)** was implemented. Excitatory interconnected neurons (blue) forming five layers of four neurons each and one inhibitory neuron (red) that makes connections to all of them, except with the four first neurons that receive external stimulation. The network projects to an output neuron (green).

Figure 2.(a) Scheme of neuron soma**,** including voltage-gated channels, Na/K-pump, cotransporters KCC and NKCC and exchangers.**(b)** Scheme of the non-synaptic mutual influence of two adjacent neuronal cells and the respective extracellular space. The local ionic changes of a neuron in the corresponding extracellular compartment electrodiffuses to the neighboring extracellular space.**(c)** Scheme of synaptic transmission in 8 steps: 1) depolarization, 2) calcium channel opening, 3) vesicle release of neurotransmitters, 4) binding to receptors of post-synaptic neuron, 5) modulation of permeability in the post-synaptic neuron, 6) neurotransmitter recapture by an enzyme, 7) storage in vesicles, 8) uptake of calcium.

Figure 3. Time course of simulation. After the initialization of the network, each stimulation pattern from the dataset is applied during 150ms, followed by

150ms of non-stimulation to let the network come back to equilibrium. Then, the synaptic weights are updated.

Figure 4. Learning in a biophysical neural tissue model. (a) Times series of membrane potentials of neurons during a simulation. **(b)** Time series of excitatory pyramidal neurons after convergence; different electrophysiological patterns can be observed: spike, spike train, burst. **(c)** Median number of epochs to converge (NEC) with median absolute deviation for different conditions: C1: biophysical network with only synaptic communication. C2: introducing variability in the synaptic network initialization. C3: adding variability to synapse initialization. C4: adding a homogeneous effect of electrodiffusion (ED). C5: introducing variability in the neural tissue (tortuosity). Confirming fast learning in cell assembly. Introduction of homogeneous ED, making the convergence slower; introducing tortuosity permits a drastic diminution of NEC.

Figure 5. Synchrony and number of epochs to converge in phenomenological models. Each orange dot represents the number of epochs to converge and the maximal value of synchrony in a generated network. In blue, mean and standard deviation for bins of 40 simulations. **(a)**Results for networks of neurons producing only spikes; **(b)** networks producing only bursts;**(c)** networks with non-synaptic influence from neurons to their neighbors; **(d)** randomly initialized network with some neurons producing only spikes and others only bursts.**(e)**For comparison, the realistic SNN in case C5, see Figure 3, is shown when neurons exhibit bursts, an activity that emerged from the non-synaptic interaction between neurons, which is the closest to the condition shown in (c).

Figure 6: Orientation detection and separation of two classes tasks.(a) – left - Horizontal and vertical separation task with 9 inputs. Histogram for 1000simulations of the number of epochs to converge to separate the 2 classes with no error: red shows the condition taking into account the non-synaptic influence, and blue shows the condition with only synaptic communication. **(a)– right** - Histogram shows the proportion of networks in the corresponding interval of the level of synchronism. **(b) – left** -Pattern recognition of handwritten 0 and 1numbers, extracted from an online UCI repository with 64 inputs. Error rate observed for 100 simulations (central line: mean, blue lines: mean and max values), depending on the number of epochs: red takes into account non-synaptic influence, while blue considers with only synaptic communication. Fewer than 10% of errors are observed

under the dashed line. **(b) – right -** Histogram shows the proportion of networks in the corresponding interval of the level of synchronism.

Figure 1

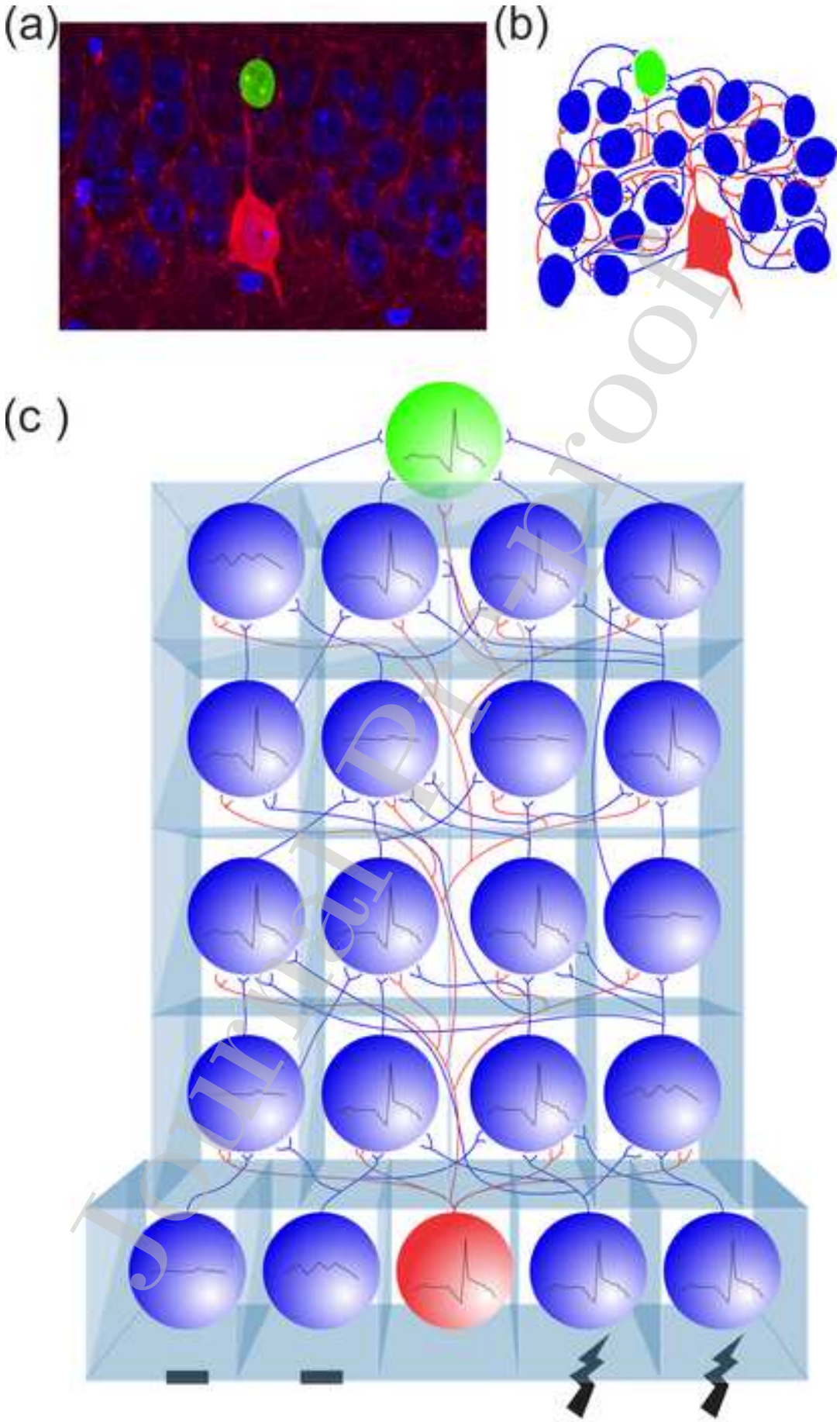

Figure 2

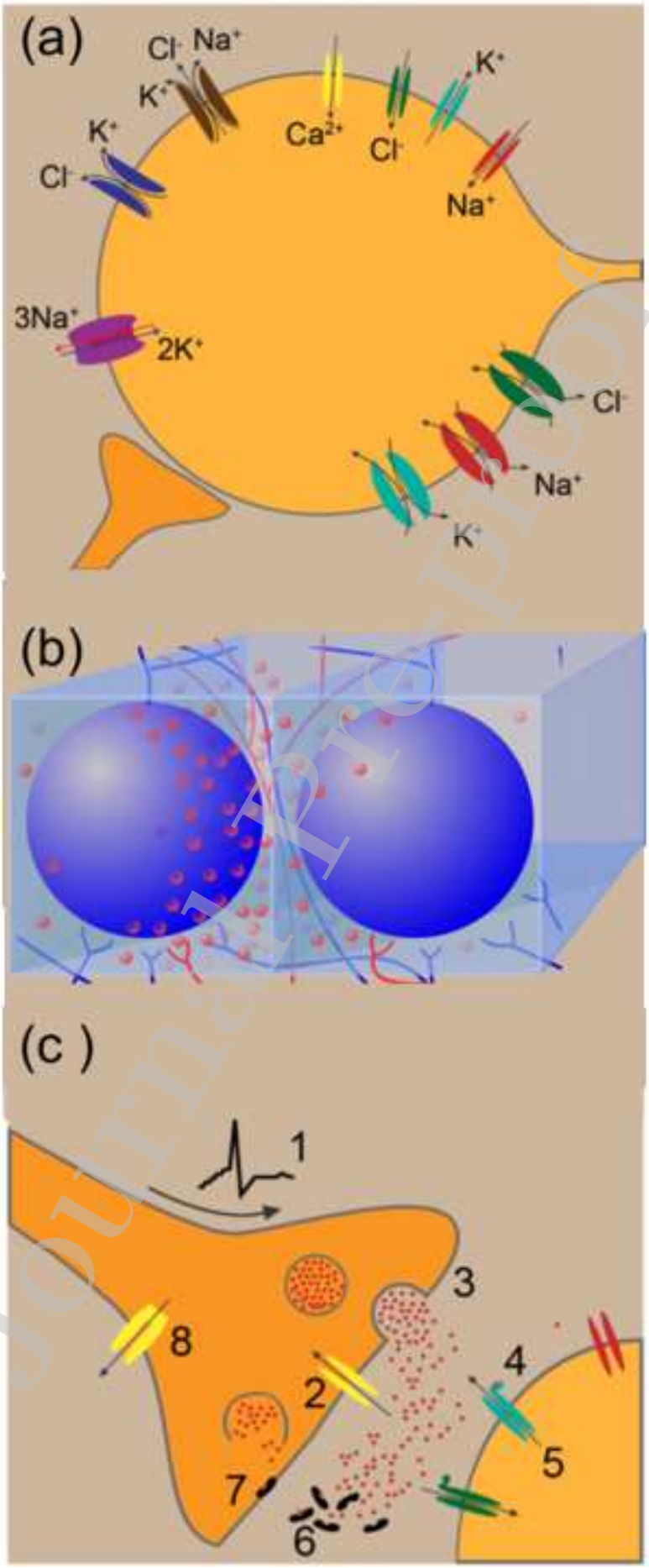

Figure 3

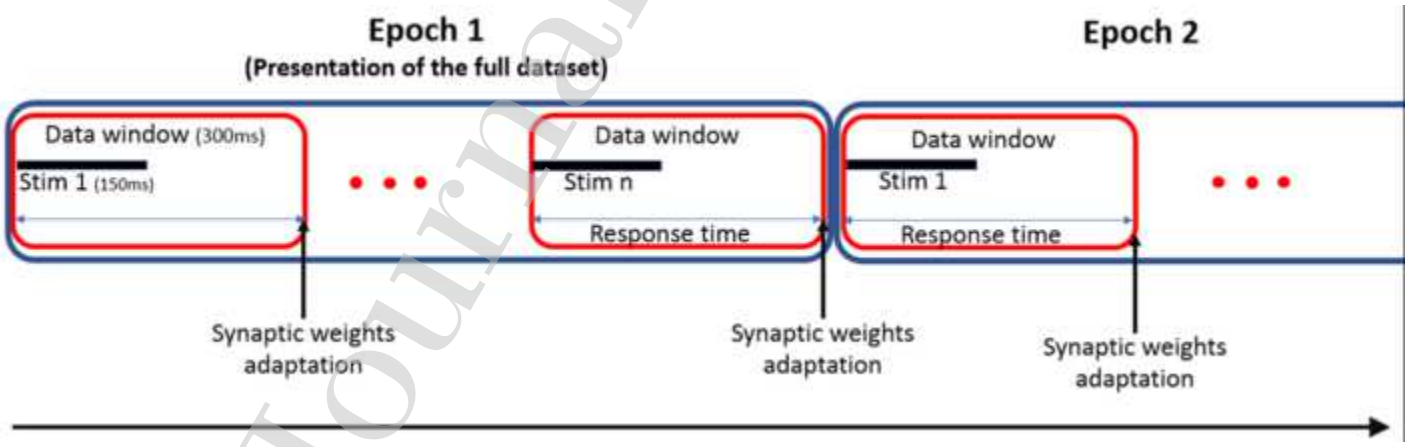

Figure 4

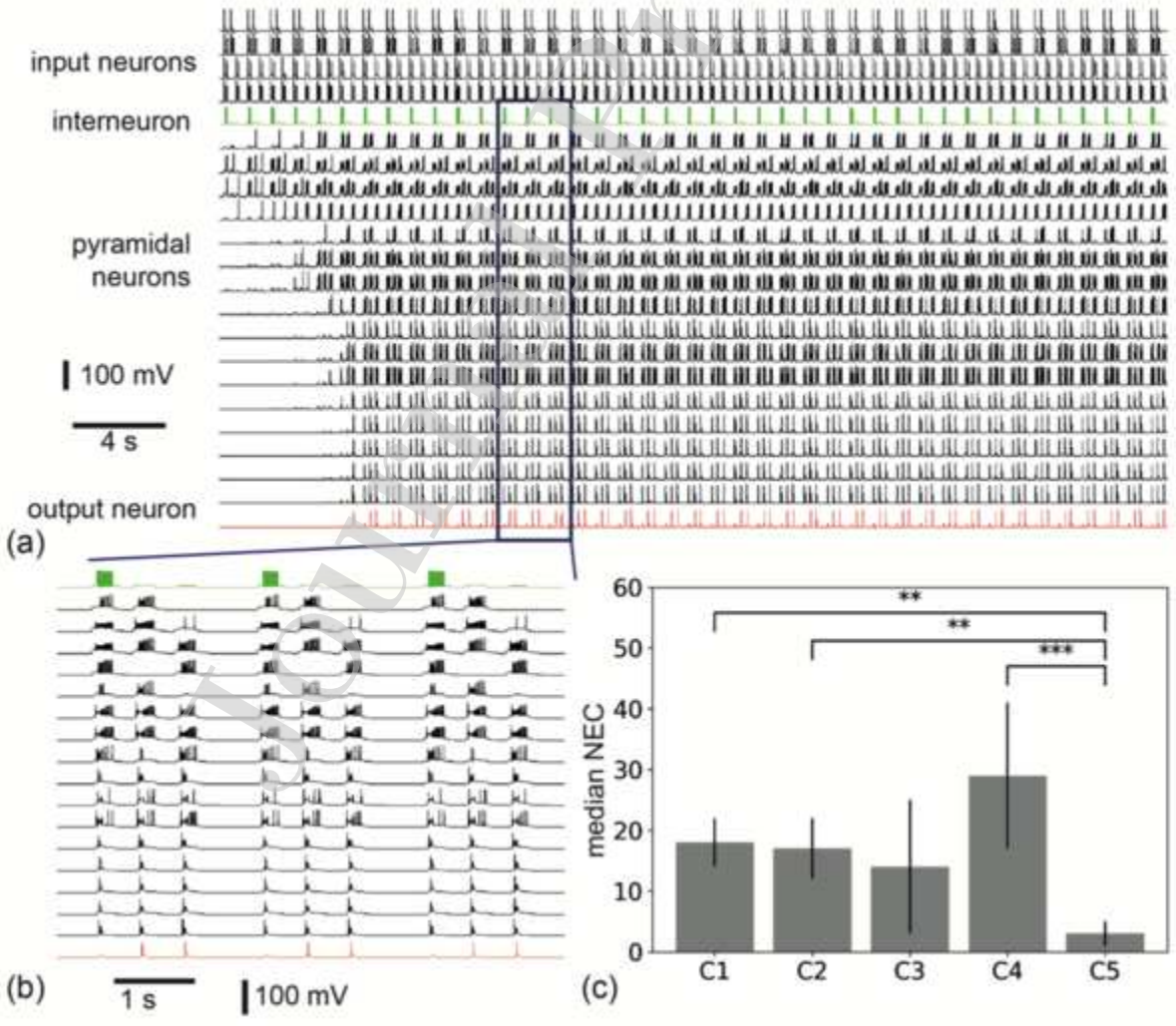

Figure 5

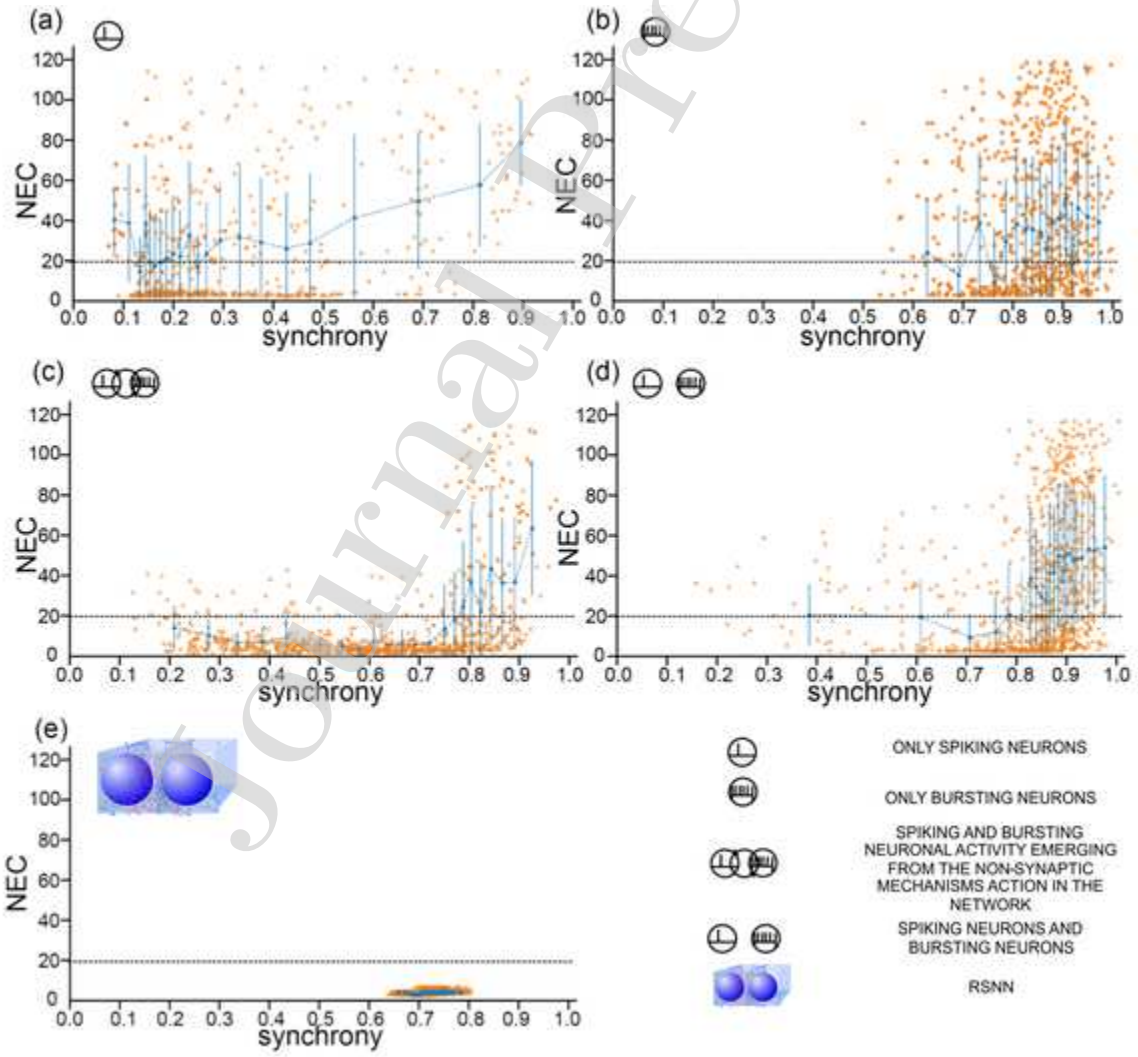

Figure 6

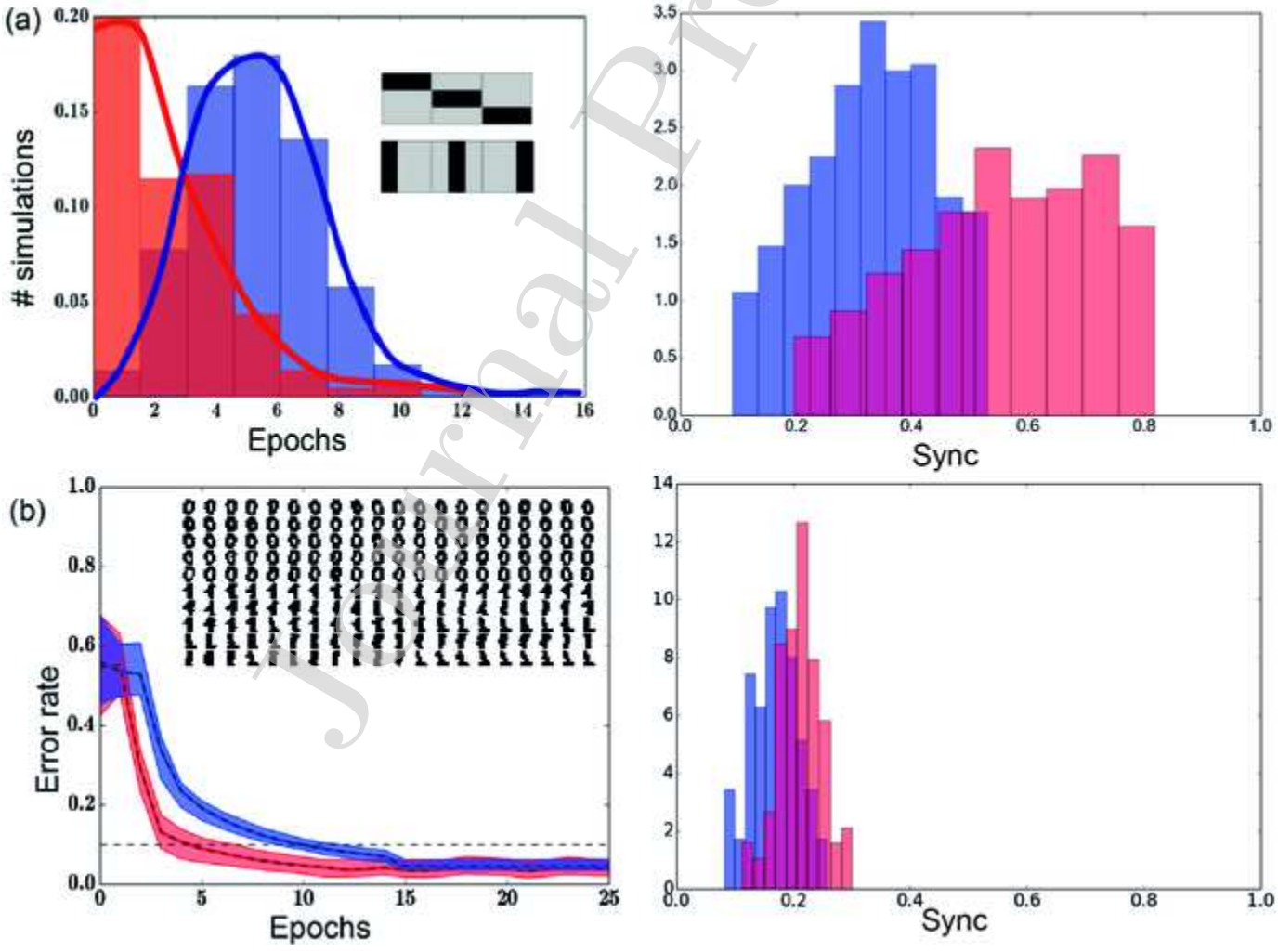

CONFLICT OF INTEREST

The submitted manuscript has been read and approved by all signatories and all authors acknowledge that they have exercised due care in ensuring the integrity of the work, and declare no conflict of interests. None of the original material contained in the manuscript has been submitted for consideration nor will any of it be published elsewhere.

São João del-Rei, june 23rd, Brazil

Antônio-Carlos Guimarães de Almeida (signed in the name of all authors)
Laboratory of Computational and Experimental Neuroscience
Biosystems Engineering Department

CONFLICT OF INTEREST

The submitted manuscript has been read and approved by all signatories and all authors acknowledge that they have exercised due care in ensuring the integrity of the work, and declare no conflict of interests. None of the original material contained in the manuscript has been submitted for consideration nor will any of it be published elsewhere.

São João del-Rei, june 23rd, Brazil

Antônio-Carlos Guimarães de Almeida (signed in the name of all authors)
Laboratory of Computational and Experimental Neuroscience
Biosystems Engineering Department